JOURNAL OF AGRICULTURAL AND FOOD CHEMISTRY

Article

pubs.acs.org/JAFC

One-Step Fabrication of a Multifunctional Magnetic Nickel Ferrite/Multi-walled Carbon Nanotubes Nanohybrid-Modified Electrode for the Determination of Benomyl in Food

Qiong Wang, Jichun Yang, Yuanyuan Dong, and Lei Zhang*

College of Chemistry, Liaoning University, 66 Chongshan Middle Road, Shenyang, Liaoning 110036, People's Republic of China

ABSTRACT: Benomyl, as one kind of agricultural pesticide, has adverse impact on human health and the environment. It is urgent to develop effective and rapid methods for quantitative determination of benomyl. A simple and sensitive electroanalytical method for determination of benomyl using a magnetic nickel ferrite ($NiFe_2O_4$)/multi-walled carbon nanotubes (MWCNTs) nanohybrid-modified glassy carbon electrode (GCE) was presented. The electrocatalytic properties and electroanalysis of benomyl on the modified electrode were investigated by cyclic voltammetry (CV) and differential pulse voltammetry (DPV). In the phosphate-buffered saline (PBS) of pH 6.0, this constructed biosensor exhibited two linear relationships with the benomyl concentration range from 1.00×10^{-7} to 5.00×10^{-7} mol/L and from 5.00×10^{-7} to 1.00×10^{-5} mol/L, respectively. The detection limit was 2.51×10^{-8} mol/L (S/N = 3). Moreover, the proposed method was successfully applied to determine benomyl in real samples with satisfactory results. The $NiFe_2O_4$/MWCNTs/GCE showed good reproducibility and stability, excellent catalytic activity, and anti-interference.

KEYWORDS: *benomyl, $NiFe_2O_4$ nanoparticles, multi-walled carbon nanotubes, cyclic voltammetry*

1. INTRODUCTION

The fungicide benomyl, i.e., methyl 1-(butylcarbamoyl)-2-benzimidazole carbamate, is a synthetic benzimidazole. It is known to exert selective toxicity against fungal cells because of its higher affinity for fungal tubulin than mammalian tubulin.[1] Benomyl is widely used for sterilizing seeds of vegetables as an agricultural chemical against a range of fungal diseases.[2,3] Because of the occurrences of benomyl and carbendazim in the environment and the potential exposure to them through diet, there continues to be ongoing concern over the risks to human health of these fungicides.[4−7] Numerous studies have been conducted to determine the fate of benomyl and its associated residues in soils, plants, and mammals.[8] Further, in mammals, benomyl is known for its ability to induce structural changes in the chromosomes and hepatocyte microtubule cytoskeleton,[9] inhibit protein synthesis[10] and lipid peroxidation, and cause glutathione depletion.[11] Recently, benomyl and carbendazim were reported as endocrine disruptors that increased both expression and activity of aromatase in the human ovarian granulose-like tumor cell line KGN.[12] There has been concern that this compound might influence human health and cause diseases. Further, benomyl is quite unstable, and it decomposes in aqueous solutions into more stable compounds, such as carbendazim and *N*,*N*′-dibutyl urea.[13,14] The determination of benomyl residue in vegetables, fruits, and environmental water samples is a difficult task. To protect consumers from the risk related to benomyl in food and environmental water, the development of a simple, rapid, and reliable method for the determination of benomyl is of great importance.

Thus far, various techniques for the detection of benomyl have been reported in the literature, such as high-performance liquid chromatography (HPLC),[15] frequency domain fluorescence,[16] fluorescence polarization,[17,18] and in-layer chromatography[19] methods. These methods have high accuracy, well reproducibility, and reliable ability of qualitative analysis. However, these methods also suffer from some disadvantages, such as expensive experimental instruments, sophisticated laboratory procedures, trained personnel, and complex sample pretreatment. In comparison to other techniques, electrochemical methods have aroused great interests among researchers because of their relatively high sensitivity, fast response, and ability to be miniaturized.[20] The literature reported that the OV-17 silicon-modified carbon paste electrodes and bare glassy carbon electrode (GCE) were used in the determination of benomyl by differential pulse voltammetry,[21,22] and the detection limit was 6.9×10^{-5} and 1.5×10^{-4} g/L, respectively. Recently, the electroanalysis method is reported for the determination of benomyl by square-wave adsorptive stripping voltammetry,[23] and the detection limit was 2.4×10^{-5} g/L. According to our knowledge, magnetic nickel ferrite/multi-walled carbon nanotubes nanohybrid-modified glassy carbon electrode ($NiFe_2O_4$/MWCNTs/GCE) for determination of benomyl had not been reported. The main objective of this paper is to develop a new method with high sensitivity, simplicity, and efficiency for the detection of benomyl.

In this paper, $NiFe_2O_4$/MWCNTs nanohybrids were synthesized through a one-step hydrothermal method and employed as a modified electrode material for the analysis of benomyl. This method is based on the different properties of the mediators plus nanoparticles, such as strong adsorptive ability, huge specific area, and subtle electronic properties.[24−26] In addition, Ni and Fe have excellent electrocatalytic activity in

Received: February 25, 2015
Revised: April 20, 2015
Accepted: April 27, 2015

DOI: 10.1021/acs.jafc.5b00973
J. Agric. Food Chem. XXXX, XXX, XXX−XXX

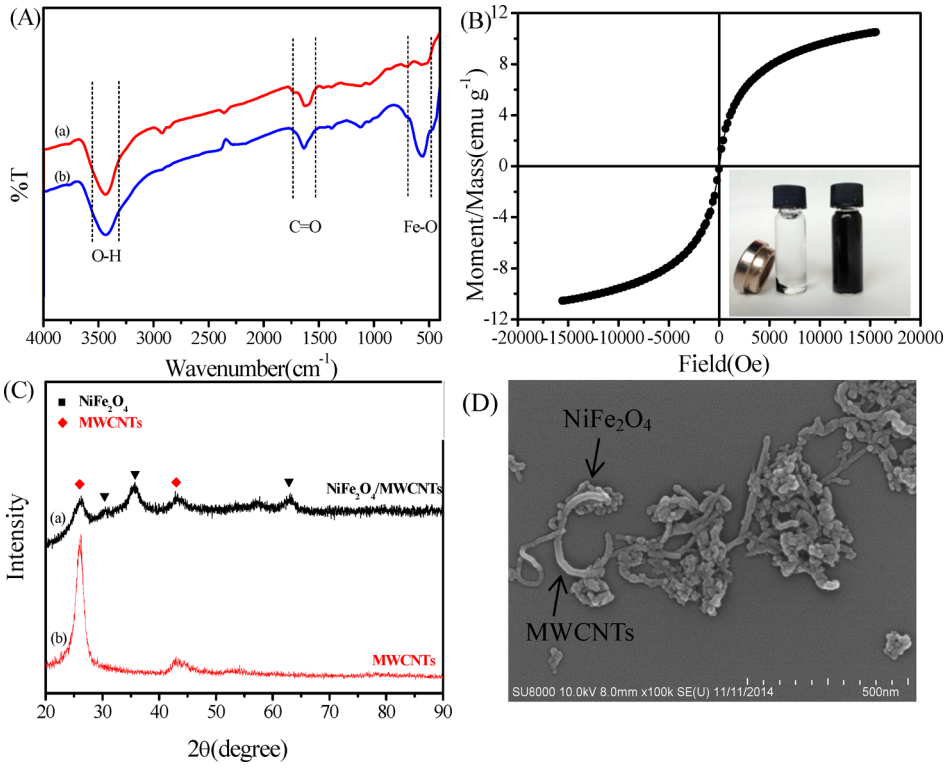

Figure 1. Characterization of MWCNTs and $NiFe_2O_4$/MWCNTs: (A) FTIR spectra of (a) MWCNTs and (b) $NiFe_2O_4$/MWCNTs, (B) VSM image of $NiFe_2O_4$/MWCNTs, (C) XRD patterns of (a) $NiFe_2O_4$/MWCNTs and (b) MWCNTs, and (D) SEM image of $NiFe_2O_4$/MWCNTs.

the catalyst of reactions of organic materials based on their electronic arrangement.[27,28] The results showed that the proposed method is simple, rapid, sensitive, and selective for the quantitative determination of benomyl at the $NiFe_2O_4$/MWCNTs/GCE.

2. EXPERIMENTAL SECTION

2.1. Chemicals and Reagents. MWCNTs (length, 0.5−2.0 μm; specific surface area, >500 m^2/g; outer diameter, <8 nm; and 95% purity) were purchased from Chengdu Organic Chemicals Co., Ltd., Chinese Academy of Sciences, Beijing, China. Benomyl (95% purity) was purchased from HEOWNS Biochemical Technology Co., Ltd. (Tianjin, China). The 5% Nafion ethanol solution (D520) was from HESEN Co., Ltd. (Shanghai, China). All other chemicals were of analytical reagent grade and produced by Shenyang Chemical Company, China.

2.2. Apparatus. A CHI660D electrochemical workstation (Shanghai ChenHua Instruments Co., China) coupled with a conventional three-electrode cell, including a platinum wire auxiliary electrode, a saturated calomel reference electrode (SCE), and a working electrode, was used for electrochemical measurements. X-ray diffraction patterns were recorded on a X-ray diffractometer (XRD, Siemens D5000, Germany) at 40 kV and 150 mA with Cu Kα radiation. The diffraction data were recorded for 2θ angles between 20° and 90°. Fourier transform infrared spectroscopy (FTIR, Avatar 330, Nicolet, Thermo Electron Scientific, Madison, WI) was used to characterize MWCNTs and $NiFe_2O_4$/MWCNTs within a 500−4000 cm^{-1} spectral domain with a resolution of 4 cm^{-1} using a KBr pellet technique at room temperature. A vibrating sample magnetometer (VSM, Lake Shore 7407, Lake Shore Cryotronics, Inc., Westerville, OH) was used to measure the magnetic prosperities of $NiFe_2O_4$/MWCNTs in the field of ±15 kOe at room temperature. The morphologies and microstructures of the material were characterized using scanning electron microscopy (Hitachi SU8000, Japan) under the voltage of 10.0 kV. A S-3C model pH meter (Shanghai Precision Scientific Instrument Co., China) was used for measuring the pH of solutions. Deionized water used throughout experiments was purified using a Sartorius Arium 611 system (Sartorius, Göttingen, Germany).

2.3. Synthesis of $NiFe_2O_4$/MWCNTs. The $NiFe_2O_4$/MWCNTs composite was fabricated by a one-step hydrothermal method. Briefly, 2.0193 g of $Fe(NO_3)_3 \cdot 9H_2O$ (0.005 mol) and 0.7017 g of $NiSO_4 \cdot 7H_2O$ (0.0025 mol) were dissolved in 50 mL of ethanol, and subsequently, 0.5 g of MWCNTs was added. Prior to that, MWCNTs were acidified with HNO_3. The obtained mixture was stirred vigorously for 1.0 h to obtain a homogeneous black solution. Then, it was transferred into a 100 mL Teflon-lined stainless-steel autoclave, heated to 180 °C, and reacted for 12 h. After that, the magnetic composite was separated by a magnet, washed repeatedly with deionized water until neutrality, and then dried at 60 °C for 12 h.

2.4. Preparation of a $NiFe_2O_4$/MWCNTs-Modified Electrode. Before modification, the bare GCE was carefully polished with three grades of alumina slurrys (0.05, 0.30, and 1.00 mm) on polishing cloth, respectively, rinsed thoroughly with deionized water between each polishing step, then washed successively with deionized water, anhydrous alcohol, and deionized water in an ultrasonic bath, and dried in air. A 4 mg/mL $NiFe_2O_4$/MWCNTs dispersion was prepared by dissolving 8.0 mg of $NiFe_2O_4$/MWCNTs in 2 mL of 1% Nafion solution prepared in ethanol. The mixture was then sonicated for 30 min to obtain a stable and well-distributed $NiFe_2O_4$/MWCNTs/Nafion suspension. A 6.0 μL drop of 4.0 mg/mL $NiFe_2O_4$/MWCNTs/Nafion suspension solution was coated on the surface of the GCE, and then the solvent was evaporated under the infrared lamp to obtain the $NiFe_2O_4$/MWCNTs/GCE.

2.5. Procedure for Benomyl Analysis. The electrochemical behavior of benomyl was studied by cyclic voltammetry (CV), and the determination of benomyl was performed by differential pulse voltammetry (DPV). All of the experiments were carried out in a conventional electrochemical cell holding 5.00 mL of 0.2 mol/L phosphate-buffered saline (PBS) at pH 6.0 and a certain amount of benomyl at room temperature. Before benomyl analysis, the 5 mL PBS solution was purged with highly purified nitrogen for 10 min.

2.6. Real Samples. Three samples of apple, mushroom, and spinach were bought in a local supermarket. Suitable amounts of three

DOI: 10.1021/acs.jafc.5b00973
J. Agric. Food Chem. XXXX, XXX, XXX−XXX

kinds of samples were added to a 50.00 mL beaker; then a suitable amount of ethanol was added to dissolve them for 30 min with ultrasonic assistance; and sample solutions were filtrated. All of the above sample solutions were stored in a refrigerator at 4 °C and determined by DPV according to the standard addition method.

3. RESULTS AND DISCUSSION

3.1. Characterization of the $NiFe_2O_4$/MWCNTs Electrode. Curve a in Figure 1A is the FTIR spectra of MWCNTs. Two characteristic peaks of MWCNTs were observed at 1650 and 3430 cm^{-1} corresponding to C═O and O−H band stretching vibrations.[29] Curve b in Figure 1A displays the FTIR spectra of the $NiFe_2O_4$/MWCNTs nanohybrid sample. The new characteristic peak at around 556 cm^{-1} is associated with the Fe−O−Ni stretching vibration.[30] This evidence confirmed that $NiFe_2O_4$ was successfully loaded to MWCNTs. Figure 1B presents the magnetic properties of $NiFe_2O_4$/MWCNTs analyzed by room-temperature VSM with an applied field of $-15.0 \leq H \leq 15.0$ kOe. The value of saturation magnetization (Ms) is about 10.48 emu g^{-1} (inset is the photo of magnetic separation).

The XRD patterns of $NiFe_2O_4$/MWCNTs and pure MWCNTs are shown in Figure 1C. The peaks at 25.9° and 43.2° were attributed to the characteristic peaks of MWCNTs (which can be seen in both curves a and b in Figure 1C).[31] Besides, from curve b in Figure 1C, it could be seen that the diffraction peaks of $NiFe_2O_4$ could be assigned to spinel-type $NiFe_2O_4$ [Joint Committee on Powder Diffraction Standards (JCPDS) 54-0964]. The peaks at the 2θ values of 30.2, 35.5, and 62.4 could be indexed to (220), (311), and (440) crystal planes of spinel $NiFe_2O_4$, respectively. The results indicated that $NiFe_2O_4$ was successfully loaded to MWCNTs.

The morphology of $NiFe_2O_4$/MWCNTs was investigated by scanning electron microscopy (SEM). From Figure 1D, it is observed that $NiFe_2O_4$ nanoparticles were deposited on the surface of MWCNTs.

3.2. Electrochemical Characterization of Benomyl. The CV behavior of benomyl on the bare GCE, $NiFe_2O_4$/GCE, MWCNTs/GCE, and $NiFe_2O_4$/MWCNTs/GCE are illustrated in Figure 2 (curves a, b, c, and d, respectively). As seen, no visible signal was found on the bare GCE (curve a), only a small and broad redox peaks of benomyl occur on the $NiFe_2O_4$/GCE (curve b) and the MWCNTs/GCE (curve c). Meanwhile, a pair of well-defined and quasi-reversible redox peaks was observed at $NiFe_2O_4$/MWCNTs/GCE (curve d), which indicates that the electrochemical reaction of benomyl is a reversible process, and the $NiFe_2O_4$/MWCNTs composite has a strong enhancement ability for the electric signal of benomyl.[32,33] This is most likely to be attributed to the large surface area of $NiFe_2O_4$/MWCNTs, which may provide many favorable sites for electron transfer to molecules, and the $NiFe_2O_4$/MWCNTs nanohybrid has a good synergic effect,[34−36] which may be ascribed to the specific and preferable properties of the magnetic nanoparticles and MWCNTs.

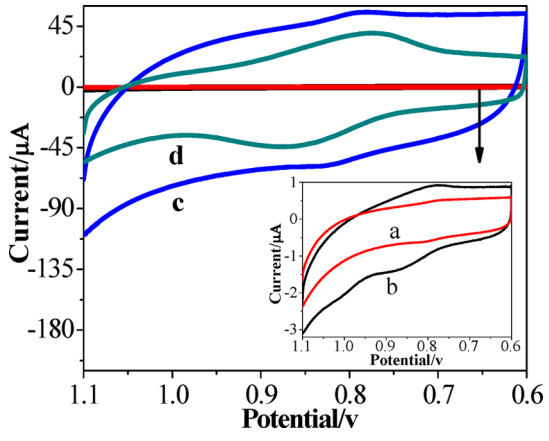

Figure 2. CVs of benomyl in 0.2 mol/L PBS at pH 6.0 solution ($C_{benomyl} = 3.5 \times 10^{-6}$ mol/L). (Inset) (a) benomyl on the bare GCE, (b) benomyl on the $NiFe_2O_4$/GCE, (c) benomyl on the MWCNTs/GCE, and (d) benomyl on the $NiFe_2O_4$/MWCNTs/GCE. Scan rate, 0.1 V/s; quiet time, 600 s.

3.3. Effect of the Modifier Amount on the Oxidation Peak Current. From the experiment, it was found that the redox peak current increased significantly with the amount of modifier (4.0 mg/mL $NiFe_2O_4$/MWCNTs/Nafion suspension solution) increasing from 4.0 to 6.0 μL, and when the amount of the suspension exceeded 6.0 μL, the current decreased. It was ascribed that the active sites for the accumulation of benomyl increased with the increment of modifier amount. The peak current decreased when the volume exceeded 6.0 μL, because the conductivity of the electrode reduced, and the film unstable as $NiFe_2O_4$/MWCNTs could leave off the electrode surface when the film was too thick. Thus, the modifier amount of 6.0 μL was chosen in the experiment.

3.4. Effect of the Accumulation Time. It is important to fix the accumulation time when adsorption studies were undertaken. Bearing this in mind, the effect of the accumulation time has been studied by the DPV method. The accumulation time can improve the amount of benomyl adsorbed on the electrode surface, then improve determination sensitivity, and decrease the detection limit. The DPV peak currents increase rapidly with the increase of the accumulation time from 0 to 600 s. However, for a longer accumulation time, there is no significant increase in the current response. This phenomenon could be attributed to the saturated adsorption of benomyl at the electrode surface. Thus, the accumulation time of 600 s was chosen in the experiment.

3.5. Effect of the pH. The effect of solution pH on the redox peak of benomyl on $NiFe_2O_4$/MWCNTs/GCE investigated at the pH range from 4.0 to 8.0 by CV is shown in Figure 3. As seen, with increasing the pH, the peak currents of benomyl increased and the potentials shifted negatively because of the participation of protons in the electrode reaction. The potentials of benomyl followed the linear regression equations with pH: E_{pa} (V) = −0.060pH + 1.14 (r = 0.9992). The value of the slope was 0.060 pH^{-1}, which is approximately close to the theoretical value of 0.0585 pH^{-1}; therefore, it can be deduced that the proton number is equal to that of the number of transferred electrons. The peak currents of benomyl increase from pH 4.0 and reach a maximum value at pH 6.0; therefore, a pH of 6.0 was chosen for the subsequent analytical experiments.

3.6. Electrochemical Properties of Benomyl. Useful information involving the electrochemical mechanism can generally be acquired from the relationship between the peak current and scan rate.[37,38] Therefore, CVs of benomyl on $NiFe_2O_4$/MWCNTs/GCE with different scan rates ranging from 0.050 to 0.20 V/s in PBS at pH 6.0 were recorded, and results are shown in Figure 4. It can be found that the peak current increased linearly with the scan rate in the range of 0.050−0.20 V s^{-1} (as shown in Figure 4A). The linear regression equations were expressed as follows: I_{pc} (μA) = 100.15v (V/s) − 4.83 (r = 0.996) and I_{pa} (μA) = −132.13v (V/

DOI: 10.1021/acs.jafc.5b00973
J. Agric. Food Chem. XXXX, XXX, XXX−XXX

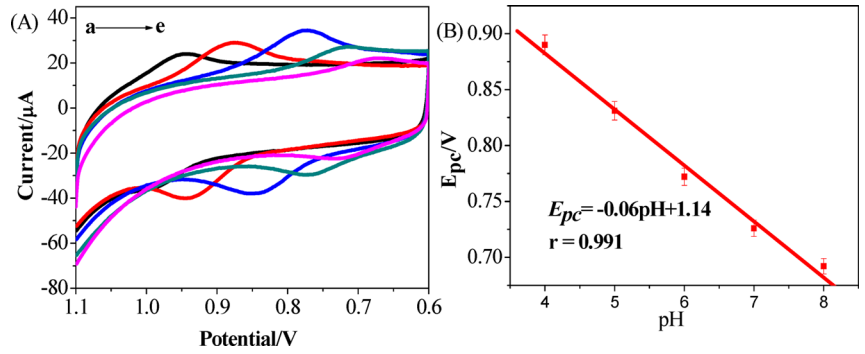

Figure 3. (A) Influence of pH on CVs of benomyl at the $NiFe_2O_4$/MWCNTs/GCE, with the pH range from a to e being 4.0−8.0, at the scan rate of 0.1 V/s, and (B) effects of pH on the potential response.

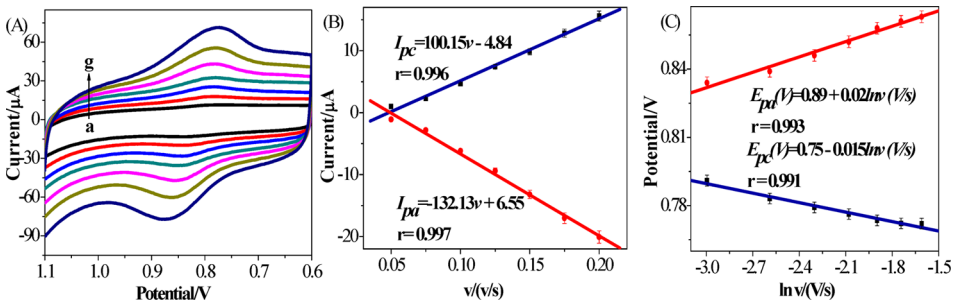

Figure 4. CVs of benomyl at different scan rates, with benomyl at 3.5×10^{-6} mol/L. (A) Scan rates from a to g are 0.050, 0.075, 0.10, 0.125, 0.15, 0.175, and 0.20 V/s, respectively. (B) Dependence of the peak current on the scan rate. (C) Dependence of the plots of E_p versus ln v.

s) + 6.55 (r = 0.997) (as shown in Figure 4B), respectively. It indicates that the redox of benomyl on $NiFe_2O_4$/MWCNTs/GCE is an adsorption-controlled process.[39,40] The ratio of the redox peak current (I_{pa}/I_{pc}) was approximately found to be 1, suggesting that the redox reaction of benomyl on $NiFe_2O_4$/MWCNTs/GCE was a quasi-reversible electrochemical behavior. In this work, the scan rate was chosen as 0.10 V s^{-1}. For an adsorption-controlled and quasi-reversible electrode process, the relationship between peak potentials and the scan rate follows Laviron's equation[41,42]

$$E_{pc} = E^0 - \frac{RT}{anF} \ln v \quad (1)$$

$$E_{pa} = E^0 + \frac{RT}{(1-a)nF} \ln v \quad (2)$$

$$\log K_s = a \log(1-a) + (1-a)\log a - \log \frac{RT}{nFv} - \frac{(1-a)anF\Delta E_p}{2.3RT} \quad (3)$$

where E_{pa} and E_{pc} are the anodic and cathodic peak potentials (V), E^0 is the formal potential (V), n is the number of electron transferred, α is the electron transfer coefficient, K_s is the standard rate constant of the surface reaction (s^{-1}), v is the scan rate (V/s), ΔE_p is the peak−peak potential separation, R is the universal gas constant (8.314 J mol^{-1} K^{-1}), T is the temperature (298 K), and F is the Faraday constant (96 500 C/mol). Figure 4C shows the plots of E_p versus ln v; the equations of the straight line were as follows: E_{pc} (V) = 0.75 − 0.015 ln v (V/s) (r = 0.991), and E_{pa} (V) = 0.87 + 0.020 ln v (V/s) (r = 0.993). The values of α and n can be determined from the slope, respectively. The electron transfer number n is close to 2, and the value of α is 0.528. Moreover, the values of K_s were calculated to be 0.951 s^{-1}. The pH effect on E_{pa} demonstrated that the number of electrons and protons involved in the benomyl oxidation process is equal (see section 3.3). Therefore, the redox of benomyl on $NiFe_2O_4$/MWCNTs/GCE is proven participation of a two protons ($2H^+$) and two electron ($2e^-$) process. The mechanism of the electrode process could be described as follows (Scheme 1).

Scheme 1. Proposed Mechanism of Electroreduction of Benomyl on the $NiFe_2O_4$/MWCNTs/GCE

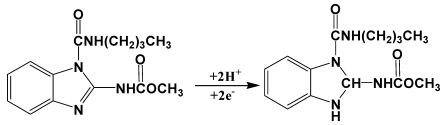

3.7. Estimation of Electrode Real Surface Areas and Γ_s.

The electrochemically effective surface areas of bare GCE and $NiFe_2O_4$/MWCNTs/GCE were determined by the chronocoulometric method according to the formula given by Anson[43]

$$Q(t) = \frac{2nFAcD^{1/2}t^{1/2}}{\pi^{1/2}} + Q_{dl} + Q_{ads} \quad (4)$$

where A is surface area of the working electrode, c is the concentration of the substrate, D is the diffusion coefficient, Q_{dl} is the double-layer charge, and Q_{ads} is the Faradaic charge. Other symbols have their usual meanings. A 0.1 mM $K_3[Fe(CN)_6]$ solution containing 1 mM KCl has a D[44] of $K_3[Fe(CN)_6]$ of 7.60×10^{-6} cm^2 s^{-1}. According to the experimental results (as shown in panels A and B of Figure 5), on the basis of the slope of the linear relationship between Q

DOI: 10.1021/acs.jafc.5b00973
J. Agric. Food Chem. XXXX, XXX, XXX−XXX

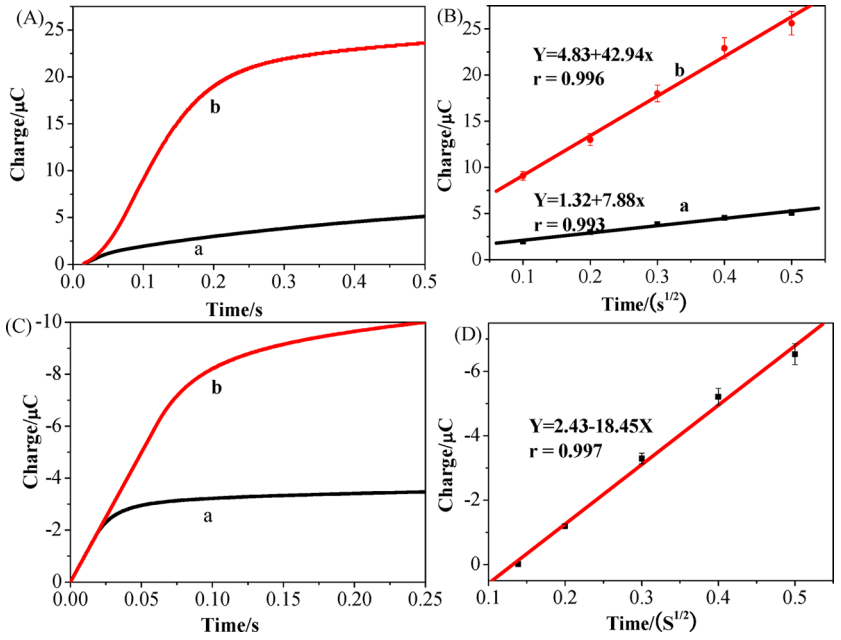

Figure 5. (A) Plot of $Q-t$ curves of (a) GCE and (b) $NiFe_2O_4$/MWCNTs/GCE in 0.1 mM $K_3[Fe(CN)_6]$ containing 1 M KCl. (B) Plot of $Q-t^{1/2}$ curves on (a) GCE and (b) $NiFe_2O_4$/MWCNTs/GCE). (C) Plot of $Q-t$ curves of the modified electrode in 0.2 M PBS at pH 6.0 in the (a) absence and (b) presence of 3.5×10^{-6} mol/L benomyl. (D) Plot of $Q-t^{1/2}$ curve on $NiFe_2O_4$/MWCNTs/GCE after the background is subtracted.

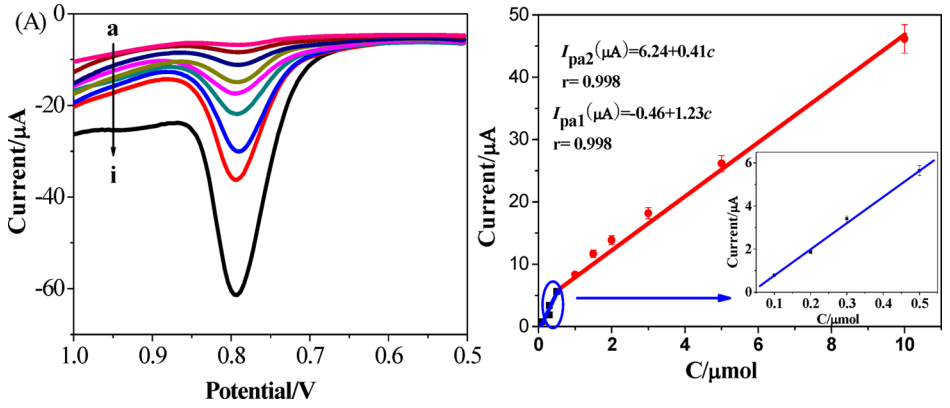

Figure 6. (A) DPVs of benomyl at different concentrations. The concentrations of benomyl from a to l are 1×10^{-7}, 2×10^{-7}, 3×10^{-7}, 5×10^{-7}, 1×10^{-6}, 1.5×10^{-6}, 3×10^{-6}, 5×10^{-6}, 1×10^{-5} mol/L, respectively. (B) Related calibration curve.

Table 1. Comparison of the Developed Method to Some Other Methods for the Determination of Benomyl

method	linear range (g/L)	detection limit (g/L)	recovery (%)	reference
liquid chromatographic	from 1.0×10^{-5} to 2.5×10^{-2}	3.3×10^{-6}		45
GC/MS	from 2.0×10^{-6} to 1.0×10^{-5}	2.0×10^{-8}	74−107	46
fluorescence polarization	from 3.0×10^{-7} to 3.0×10^{-4}	1.1×10^{-7}	104−113	47
bare GCE	from 8.1×10^{-5} to 1.5×10^{-3}	2.4×10^{-5}	99	21
OV-17 silicon-modified carbon paste electrodes	from 1.0×10^{-5} to 4.0×10^{-4}	6.9×10^{-5}	31−83	23
$NiFe_2O_4$/MWCNTs-modified GCE	from 2.9×10^{-5} to 2.9×10^{-3}	7.2×10^{-6}	93−103	present work

and $t^{1/2}$, A was calculated to be 0.013 and 0.072 cm^2 for bare GCE and $NiFe_2O_4$/MWCNTs/GCE, respectively. These results indicated that the specific area of the modified electrodes is nearly 6 times that of the bare electrode, which would enhance the current response and decrease the detection limit.

The diffusion coefficient D and Faradaic charge Q_{ads} of benomyl at $NiFe_2O_4$/MWCNTs/GCE can also be determined by chronocoulometry based on eq 4. As shown in panels C and D of Figure 5, after background subtraction, the plot of Q against $t^{1/2}$ showed a linear relationship. With $n = 2$, $A = 0.072$ cm^2, and $c = 3.5 \times 10^{-6}$ mol/L, D was calculated to be 1.13×10^{-7} cm^2 s^{-1}. According to the equation $Q_{ads} = nFA\Gamma_s$, the adsorption capacity, Γ_s, can be obtained as 1.75×10^{-10} mol cm^{-2}.

3.8. Electrochemical Determination of Benomyl Using DPV. As a highly sensitive and low detection limit electrochemical method, DPV was used for the determination of benomyl. Figure 6 presents DPV curves of benomyl at different concentrations on the $NiFe_2O_4$/MWCNTs/GCE under the

DOI: 10.1021/acs.jafc.5b00973
J. Agric. Food Chem. XXXX, XXX, XXX−XXX

optimum conditions. It can be seen that an increase in the benomyl concentration is accompanied by an increase in anodic current, but there are two linear sections in the regression line that fit the following equations: for concentrations in the range from 1.00×10^{-7} to 5.00×10^{-7} mol/L, I_{pa} (μA) = −0.46 + 1.23c (μmol/L) (r = 0.998), and for concentrations in the range from 5.00×10^{-7} to 1.00×10^{-5} mol/L, I_{pa} (μA) = 6.24 + 0.41c (μmol/L) (r = 0.995). The detection limit was 2.51×10^{-8} mol/L based on 3 times that of the background noise. It could be seen that the proposed method showed a rational linear range and an acceptable detection limit.

The comparison of the developed method to some other methods for the determination of benomyl is listed in Table 1, which showed excellent sensitivity and a wide linear range of the proposed method.

3.9. Reproducibility, Stability, and Interference Study. The $NiFe_2O_4$/MWCNTs/GCE showed good reproducibility, and the relative standard deviation (RSD) was 3.3%, which was evaluated by six repetitive measurements of 3.5×10^{-6} mol/L benomyl in PBS at pH 6.0 (accumulation time, 600 s; scan rate, 0.10 V s^{-1}; and accumulation potential, open circuit potential), which indicates that the electrochemical response of benomyl at the $NiFe_2O_4$/MWCNTs/GCE was highly reproducible. The DPV responses remained 91% of the initial current after the $NiFe_2O_4$/MWCNTs/GCE electrode was stored in a refrigerator at 4 °C for 7 days, suggesting good stability.

Under the optimized conditions, the redox peaks current of 3.5×10^{-6} mol/L benomyl was individually measured in the presence of different interferents and their influence on the analytical signal was investigated. As shown in Figure 7, it was found that 100-fold concentrations of carbendazim, thiabendazole, and tricyclazole, 300-fold concentrations of vitamin C, glucose, and CO_3^{2-}, and 1000-fold concentrations of Ca^{2+}, Mg^{2+}, K^+, Na^+, Zn^{2+}, Cl^-, and NO_3^- have no influence on the signal of benomyl. The results indicated that the peak current of benomyl was not significantly affected by the presence of common existing substances, suggesting a great anti-interference ability of the $NiFe_2O_4$/MWCNTs/GCE.

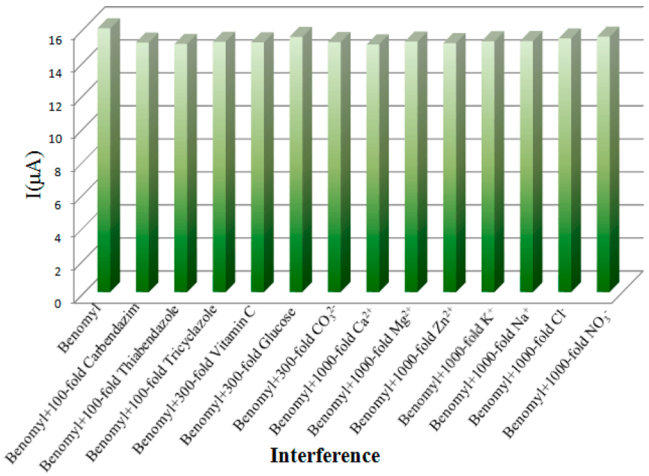

Figure 7. Signal of benomyl in the presence of interfering compounds.

3.10. Analysis of the Real Sample. To evaluate the practical application of $NiFe_2O_4$/MWCNTs/GCE for real sample analysis, apple, mushroom, and spinach were analyzed and detected by DPV under the optimal conditions using the standard addition method. The results are given in Table 2, and the recoveries were determined in the range from 93 to 103%. As indicated by the results, the developed sensor was proven to be a promising and reliable tool for the determination of benomyl in food and possesses potential applications in the analysis of the relevant real samples.

Table 2. Determination of Benomyl in Real Samples

sample	added ($\times 10^{-5}$, mol/L)	found[a] ($\times 10^{-5}$, mol/L)	RSD[b] (%)	recovery (%)
apple	0	0		
	0.482	0.479	3.5	99.3
	3.445	3.500	3.8	101.6
mushroom	0	0		
	0.482	0.496	2.6	96.9
	3.445	3.500	4.1	98.5
spinach	0	0		
	0.482	0.463	5.3	96.1
	3.445	3.211	4.5	93.2

[a]Mean of three measurement. [b]Relative standard deviation for n = 5.

4. CONCLUSION

In this work, a sensitive and reliable electrochemical method was proposed to determine benomyl. The electrochemical sensor based on $NiFe_2O_4$/MWCNTs/GCE displays an electrocatalytic performance to the oxidation of benomyl with a low detection limit. The electrochemical sensor shows good sensitivity, selectivity, and reproducibility. The $NiFe_2O_4$/MWCNTs/GCE is proven to be an accurate and reliable method because of the determination of benomyl in real samples with satisfactory results.

AUTHOR INFORMATION

Corresponding Author

*Telephone: +86-24-62207809. Fax: +86-24-62202380. E-mail: zhanglei63@126.com.

Funding

This project was supported by the National Natural Science Foundation of China (NSFC, 51178212), the Science and Technology Foundation of Ocean and Fisheries of Liaoning Province (201408 and 201406), and the Foundation of 211 Project for Innovative Talent Training, Liaoning University.

Notes

The authors declare no competing financial interest.

REFERENCES

(1) Kilmartin, J. V. Purification of yeast tubulin by self-assembly in vitro. *Biochemistry* **1981**, *20*, 3629−3633.

(2) Peres, N. A.; Timmer, L. W.; Adaskaveg, J. E.; Correll, J. C. Lifestyle of *Colletotrichum acutatum*. *Plant Dis.* **2005**, *89*, 784−796.

(3) Davidse, L. C. Benzimidazole fungicides—Mechanism of action and biological impact. *Annu. Rev. Phytopathol.* **1986**, *24*, 43−65.

(4) Rathinasamy; Panda, D. Kinetic stabilization of microtubule dynamic instability by benomyl increases the nuclear transport of p53. *Biochem. Pharmacol.* **2008**, *76*, 1669−1680.

(5) Davidse, L. C.; Flach, W. Differential binding of methyl benzimidazole-2-yl carbamate to fungal tubulin as a mechanism of resistance to this antimitotic agent in mutant strains of *Aspergillus nidulans*. *J. Cell Biol.* **1977**, *72*, 174−193.

(6) Zhou, J.; Xiong, K.; Yang, Y.; Ye, X.; Liu, J.; Li, F. Deleterious effects of benomyl and carbendazim on human placental trophoblast cells. *Reprod. Toxicol.* **2014**, *51*, 64−71.

DOI: 10.1021/acs.jafc.5b00973
J. Agric. Food Chem. XXXX, XXX, XXX−XXX

(7) Zelesco, P. A.; Barbieri, I.; Graves, J. A. M. Use of a cell hybrid test system to demonstrate that benomyl induces aneuploidy and polyploidy. *Mutat. Res., Genet. Toxicol. Test.* **1990**, *242*, 329−335.
(8) Baude, F. J.; Pease, H. L.; Holt, R. F. Fate of benomyl on field soil and turf. *J. Agric. Food Chem.* **1974**, *22*, 413−418.
(9) Urani, C.; Chiesara, E.; Galvani; Marabini, L.; Santagostino, A.; Camatini, M. Benomyl affects the microtubule cytoskeleton and the glutathione level of mammalian primary cultured hepatocytes. *Toxicol. Lett.* **1995**, *76*, 135−144.
(10) Marinovich, M.; Ghilardi, F.; Galli, C. L. Effect of pesticide mixtures on in vitro nervous cells: comparison with single pesticides. *Toxicology* **1996**, *108*, 201−206.
(11) Banks, D.; Soliman, M. R. Protective effects of antioxidants against benomyl-induced lipid peroxidation and glutathione depletion in rats. *Toxicology* **1997**, *116*, 177−181.
(12) Morinaga, H.; Yanase, T.; Nomura, M.; Okabe, T.; Goto, K.; Harada, N.; Nawata, H. A benzimidazole fungicide, benomyl, and its metabolite, carbendazim, induce aromatase activity in a human ovarian granulose-like tumor cell line (KGN). *Endocrinology* **2004**, *145*, 1860−1869.
(13) Sassman, S. A.; Lee, L. S.; Bischoff, M.; Turco, R. F. Assessing *N*,*N*′-dibutylurea (DBU) formation in soils after application of *n*-butylisocyanate and benlate fungicides. *J. Agric. Food Chem.* **2004**, *52*, 747−54.
(14) Garcia Sanchez, F.; Aguilar Gallardo, A. Fluorimetric determination of the fungicide benomyl after solvolysis. *Microchim. Acta* **1994**, *116*, 211−218.
(15) Bernal, J. L.; Nozala, M. J.; Toribio, L.; Jiménez, J. J.; Atienza, J. High-performance liquid chromatographic determination of benomyl and carbendazim residues in apiarian samples. *Journal of Chromatography A* **1997**, *787*, 129−136.
(16) Navas Díaz, A.; García Sánchez, F.; López Guerrero, M. M. Modulated anisotropy fluorescence for quantitative determination of carbaryl and benomyl. *Talanta* **2003**, *60*, 629−634.
(17) García Reyes, J. F.; Ortega Barrales, P.; Molina Díaz, A. Gel-surface enhanced fluorescence sensing system coupled to a continuous-flow assembly for simultaneous monitoring of benomyl and carbendazim. *Anal. Chim. Acta* **2003**, *493*, 35−45.
(18) García Sánchez, F.; Navas Díaz, A.; Torijas, M. C. Selective determination of carbaryl and benomyl by fluorescence polarization. *Anal. Chim. Acta* **2000**, *414*, 25−32.
(19) MacNeil, J. D.; Hikichi, M. A rapid method for the quantitive analysis of benomyl on cherries by thin-layer chromatography and in situ fluorometry. *J. Chromatogr. A* **1974**, *101*, 33−37.
(20) Zima, J.; Svancara, I.; Barek, J.; Vytras, K. Recent advances in electroanalysis of organic compounds at carbon paste electrodes. *Crit. Rev. Anal. Chem.* **2009**, *39*, 204−227.
(21) Sarigül, T.; Inam, R.; Demir, E.; Aboul-Enein, H. Y. Electro-oxidation and determination of benomyl by square-wave adsorptive stripping voltammetry. *J. AOAC Int.* **2014**, *97*, 995−1000.
(22) Muñíz Alvarez, J. L.; García Calzón, J. A.; López Fonseca, J. M. Catalytic polarographic prewave of cobalt(II) induced by carbendazim. Application to the voltammetric determination of benomyl. *Electroanalysis* **1997**, *9*, 500−502.
(23) Hernindez, P.; Garcia, S.; Hernindez, L. Voltammetric use of a graphite electrode modified with OV-17 silicone for the determination of organic compounds. *Anal. Chim. Acta* **1992**, *259*, 325−331.
(24) Shipway, A. N.; Lahav, M.; Willner, I. Nanostructured gold colloid electrodes. *Adv. Mater.* **2000**, *12*, 993.
(25) Wang, L.; Ji, H.; Wang, S.; Kong, L.; Jiang, X.; Yang, G. Preparation of Fe_3O_4 with high specific surface area and improved capacitance as a supercapacitor. *Nanoscale* **2013**, *5*, 3793.
(26) Anwar, S.; Muthu, K. S.; Ganesh, V.; Lakshminarasimhan, N. J. A comparative study of electrochemical capacitive behavior of $NiFe_2O_4$ synthesized by different routes. *J. Electrochem. Soc.* **2011**, *158*, A976−A981.
(27) Wang, R.; Xie, M.; Li, P.; Fai, N. G. Catalytic and electrocatalytic oxidation of propane on V−Mg−O and V−Mg−O (Ag) catalysts. *Catal. Lett.* **1994**, *24*, 67−77.
(28) Ehsania, A.; Vaziri-Rad, A.; Babaei, F.; Shiri, H. M. Electrosynthesis, optical modeling and electrocatalytic activity of Ni−MWCNT−PT nanocomposite film. *Electrochim. Acta* **2015**, *159*, 140−148.
(29) Gordani, G. R.; Ghasemi, A.; Saidi, A. Optimization of carbon nanotube volume percentage for enhancement of high frequency magnetic properties of $SrFe_8MgCoTi_2O_{19}$/MWCNTs. *J. Magn. Magn. Mater.* **2014**, *363*, 49−54.
(30) Cao, N.; Zou, X. Y.; Huang, Y. Q.; Zhao, Y. B. Preparation of $NiFe_2O_4$ architectures for affinity separation of histidine-tagged proteins. *Mater. Lett.* **2015**, *144*, 161−164.
(31) Chen, C. H.; Liang, Y. H.; Zhang, W. D. $ZnFe_2O_4$/MWCNTs composite with enhanced photocatalytic activity under visible-light irradiation. *J. Alloys Compd.* **2010**, *501*, 168−172.
(32) Gunjakar, J. L.; More, A. M.; Shinde, V. R.; Lokhande, C. D. Synthesis of nanocrystalline nickel ferrite ($NiFe_2O_4$) thin films using low temperature modified chemical method. *J. Alloys Compd.* **2008**, *465*, 468−473.
(33) Jauhar, S.; Singhal, S. Substituted cobalt nano-ferrites, $CoM_xFe_{2-x}O_4$ (M = Cr^{3+}, Ni^{2+}, Cu^{2+}, Zn^{2+}; $0.2 \leq x \leq 1.0$) as heterogeneous catalysts for modified Fenton's reaction. *Ceram. Int.* **2014**, *40*, 11845−11855.
(34) Xiong, P.; Hu, C. Y.; Fan, Y.; Zhang, W. Y.; Zhu, J. W.; Wang, X. Ternary manganese ferrite/graphene/polyaniline nanostructure with enhanced electrochemical capacitance performance. *J. Power Sources* **2014**, *266*, 384−392.
(35) Cai, W. H.; Lai, T.; Dai, W. L.; Ye, J. S. A facile approach to fabricate flexible all-solid-state supercapacitors based on $MnFe_2O_4$/graphene hybrids. *J. Power Sources* **2014**, *255*, 170−178.
(36) Fu, M.; Jiao, Q. Z.; Zhao, Y. In situ fabrication and characterization of cobalt ferrite nanorods/graphene composites. *Mater. Charact.* **2013**, *86*, 303−315.
(37) Zhang, Y. Y.; Hu, L. T.; Liu, X.; Liu, B. F.; Wu, K. B. Highly-sensitive and rapid detection of ponceau 4R and tartrazine in drinks using alumina microfibers-based electrochemical sensor. *Food Chem.* **2015**, *166*, 352−357.
(38) Wang, X.; Yang, J. C.; Wang, Y. J.; Li, Y. H.; Wang, F.; Zhang, L. Studies on electrochemical oxidation of estrogenic disrupting compound bisphenol AF and its interaction with human serumalbumin. *J. Hazard. Mater.* **2014**, *276*, 105−111.
(39) Yang, X.; Feng, B.; Yang, P.; Ding, Y. L.; Chen, Y.; Fei, J. J. Electrochemical determination of toxic ractopamine at an ordered mesoporous carbon modified electrode. *Food Chem.* **2014**, *145*, 619−624.
(40) Gu, X. F.; Jiang, G. M.; Jiang, G. Q.; Chen, T. T.; Zhan, W. Y.; Li, X.; Wu, S. J.; Tian, S. Detection of dopamine on a mercapto-terminated hexanuclear Fe(III) cluster modified gold electrode. *Talanta* **2015**, *137*, 189−196.
(41) Laviron, E. J. Adsorption autoinhibition and autocatalysis in polarography and linear potential sweep voltammetry. *J. Electroanal. Chem. Interfacial Electrochem.* **1974**, *52*, 355−393.
(42) Laviron, E. J. General expression of the linear potential sweep voltammogram in the case of diffusionless electrochemical systems. *J. Electroanal. Chem. Interfacial Electrochem.* **1979**, *101*, 19−28.
(43) Anson, F. C. Application of potentiostatic current integration to the study of the adsorption of cobalt(III)−(ethylenedinitrilo-(tetraacetate) on mercury electrodes. *Anal. Chem.* **1964**, *36*, 932−934.
(44) Yu, L. L.; Shi, M. X.; Yue, X.; Qu, L. B. A novel and sensitive hexadecyltrimethyl ammonium bromide functionalized graphene supported platinum nanoparticles composite modified glassy carbon electrode for determination of sunset yellow in soft drinks. *Sens. Actuators, B* **2015**, *209*, 1−8.
(45) Navickiene, S.; Possidônio de, O.; Junior, A.; Brito, N. M.; Graciolli, L. A.; Lúcia Ribeiro, M. Determination of benomyl residues in shiitake mushrooms (*Lentinula edodes*) by liquid chromatography with UV detection. *J. Chromatogr. Sci.* **2007**, *45*, 340−344.
(46) Shin, H. S.; Hong, J. E.; Pyo, H.; Park, S. J.; Lee, W. Sensitive determination of benomyl in environmental samples by GC/MSD. *Anal. Chem.* **2001**, *17*, 49−52.

DOI: 10.1021/acs.jafc.5b00973
J. Agric. Food Chem. XXXX, XXX, XXX−XXX

(47) García Sánchez, F.; Navas Díaz, A.; Torijas, M. C. Selective determination of carbaryl and benomyl by fluorescence polarization. *Anal. Chim. Acta* **2000**, *414*, 25−32.

DOI: 10.1021/acs.jafc.5b00973
J. Agric. Food Chem. XXXX, XXX, XXX−XXX